



Ethylbenzene and toluene interactions with biochar from municipal solid waste in single and dual systems

Yohan Jayawardhana^a, S. Keerthanan^b, Su Shiung Lam^c, Meththika Vithanage^{a,b,*}

^a Environmental Chemodynamics Research Group, National Institute of Fundamental Studies, Kandy, 20000, Sri Lanka

^b Ecosphere Resilience Research Centre, Faculty of Applied Sciences, University of Sri Jayewardenepura, Nugegoda, 10250, Sri Lanka

^c Higher Institution Centre of Excellence (HICoE), Institute of Tropical Aquaculture and Fisheries (AKUATROP), Universiti Malaysia Terengganu, 21030, Kuala Nerus, Terengganu, Malaysia

ARTICLE INFO

Keywords:

Municipal solid waste
Biochar
Adsorption
Volatile organic compounds
BTEX

ABSTRACT

The present study investigated adsorptive removal of toluene and ethylbenzene from the aqueous media via using biochar derived from municipal solid waste (termed “MSW-BC”) in a single and binary contaminant system at 25–45 °C. The adsorption was evaluated at different pH (3–10), experimental time (up to 24 h), and initial adsorbate concentrations (10–600 µg/L) in single and binary contaminant system. A fixed-bed column experiment was also conducted using MSW-BC (0.25%) and influent concentration of toluene and ethylbenzene (4 mg/L) at 2 mL/min of flow rate. The adsorption of toluene and ethylbenzene on the MSW-BC was mildly dependent on the pH, and the peak adsorption ability (44–47 µg/g) was recorded at a baseline pH of ~8 in mono and dual contaminant system. Langmuir and Hill are the models that match the isotherm results in a single contaminant environment for both toluene (R^2 of 0.97 and 0.99, respectively) and ethylbenzene (R^2 of 0.99 and 0.99, respectively) adsorption. In the binary system, the isotherm models matched in the order of Langmuir > Hill > Freundlich for toluene, whereas Hill > Freundlich > Langmuir for ethylbenzene. The adsorption in the batch experiment was likely to take place via cooperative and multilayer adsorption onto MSW-BC involving hydrophobic, π - π and n - π attractions, specific interaction such as hydrogen- π and cation- π interactions, and van der Waals interactions. The thermodynamic results indicate exothermic adsorption occurred by physical attractions between toluene and ethylbenzene, and MSW-BC. The breakthrough behavior of toluene and ethylbenzene was successfully described with Yoon-Nelson and Thomas models. The data demonstrate that the low-cost adsorbent derived from the municipal solid waste can be utilized to remove toluene and ethylbenzene in landfill leachate.

1. Introduction

The low-molecular-weight organic compounds that produce vapor efficiently at ambient temperatures are known as Volatile organic compounds (VOCs). These compounds are mostly anthropogenic and emitted from the industry discharge, (i.e. solvents used for chemical manufacturing, a byproduct of the combustion of petroleum products, and burning of coal), degradation and decomposition of consumer products, (i.e. pharmaceutical and personal care products, paint, degreasers, refrigerants, furniture) and landfills of municipal solid waste (MSW) (Jain et al., 2016; Kulikowska and Klimiuk 2008; Kumarathilaka et al., 2016). The most common VOCs include aliphatic and aromatic organic compounds such as methane, aldehydes, benzene, toluene, xylene, naphthalene, etc. Among the various VOCs sources to the

environment, MSW open dumpsites are considered one of the most perilous as those dumpsites emit loads of VOCs and some PAH from waste decomposition (Krcmar et al., 2018; Kumarathilaka et al., 2016; Nair et al., 2019).

Some of the VOCs can be categorized as a subgroup comprised of aromatics, including Benzene, Toluene, Ethylbenzene and Xylene (BTEX). Oil spills are one of the dominant contaminant sources for BTEX (Mitra and Roy 2011). Besides, BTEX is commonly discharged to the environment through MSW dumps or landfills. Among those, benzene, toluene and ethylbenzene are considered priority pollutants by the USEPA (Yue et al., 2001). Toluene is one of the most observed aromatic hydrocarbons in landfill leachate (Kumarathilaka et al., 2014; Meckenstock et al., 2004). However, only a few studies have assessed BTEX concentrations in MSW dumpsites, and these studies found that the

* Corresponding author. Environmental Chemodynamics Research Group, National Institute of Fundamental Studies, Kandy, 20000, Sri Lanka.
E-mail address: meththika@sjp.ac.lk (M. Vithanage).

concentration of benzene, toluene, ethylbenzene and xylene concentrations were ranged 140–9.01, 11.44–1277, 14.56–383, and 24.06–341 µg/L, respectively, in leachate from a landfill in Warmia, Poland, Denmark, Iran and Turkey (Durmusoglu et al., 2010; Kulkowska and Klimiuk 2008; Yaghmaien et al., 2019) Whereas, in Sri Lanka, the concentrations were reported as low at 21, 20, 6, and 7 µg/L (Kumarathilaka et al., 2016; Scheutz et al., 2004). Once these VOCs are mixed with groundwater, a high cost is often spent on the remediation (Zhang et al., 2016). Deep excavation and injection wells pump and treat for BTEX with combining other organics are often costly techniques and consistency maintains in the underground treatment are challenging (U.S.EPA 2001). The repercussion is that BTEX occurrences, even in trace levels in landfill environments, are potentially carcinogenic to human health (Durmusoglu et al., 2010; Yaghmaien et al., 2019). Therefore, developing effective BTEX remediation techniques is of great significance and urgent necessity, especially for most open dumpsites as BTEX could directly discharge water bodies.

BTEX removal techniques gain recent attention due to the toxicity associated with their pervasive presence in the environment. Various technologies have been employed for BTEX removal such as advanced oxidation, adsorption, phytoremediation, and photocatalysis (Yeh et al., 2010). Among those removal technologies, adsorption receives a topical focus due to the cost-effectiveness and requirement of less-skilled operation, although the cost is also governed by the material used (De Gisi et al., 2016). Moreover, modified materials have been utilized for BTEX removal in aqueous media, such as surfactant-modified zeolite, demonstrated a BTEX removal performance of 18 L/kg for benzene and 95 L/kg for p- and m-xylene (Ranck et al., 2005). Ordered mesoporous carbon delivered an overall BTEX removal capacity of 19.8 mg/g (Konggidinata et al., 2017). Non-ionic surfactant modified montmorillonite has exhibited 5.9, 6.7, 7.4, and 8.2 mg/g of removal capacity for BTEX with an overall 18.8 mg/g (Nourmoradi et al., 2012).

Recent efforts have been placed on using carbon-based resources such as activated carbon and biochar due to their high surface areas and the potential of using various waste biomasses for production (Abedinzadeh et al., 2020; Lehmann and Joseph 2015). Durian shell activated carbon used for toluene removal reported 54 mg/g as the Langmuir maximum removal capacity (Tham et al., 2011). Different types of biochars were tested against the removal of odorous VOCs emitted from the swine manure and Oakwood biochar showed the best performance over the types of biochar examined (Hwang et al., 2018; Saiz-Rubio et al., 2019). However, the removal of BTEX by municipal solid waste biochar (MSW-BC) has not been studied. Nitrogen-doped phosphates demonstrated an impressive toluene removal capacity of 496 mg/g (Zhou et al., 2018), whereas biochar produced from municipal solid waste presented rather excellent maximum removal of 850, 576 and 550 µg/g for toluene, benzene and m-xylene, respectively (Jayawardhana et al., 2019b, c, Jayawardhana et al., 2019d). The MSW-BC has received recent prospects due to the dual benefits, acting as a material for leachate treatment and waste volume reduction (Gunarathne et al., 2019; Jayawardhana et al., 2018). The MSW-BC recently utilized in the remediation of inorganic contaminants, such as heavy metals and organic contaminants, such as pharmaceutical and personal care products by various studies of Abedinzadeh et al. (2020), Ashiq et al. (2019a), and Ashiq et al. (2019b). Despite many studies on the adsorptive removal of BTEX by MSW-BC in a single contaminant environment, the studies to assess co-contaminants' influence on the adsorption behavior in a binary contaminant in aqueous media are limited in the present knowledge. And, the practical approaches of BTEX removal are based on the column studies are also inadequate. Therefore, the objectives of this research were to: (1) convert the municipal solid waste into a beneficial adsorbent and also estimate the techno-cost in preparation of MSW-BC from the waste; (2) assess toluene and ethylbenzene adsorption onto MSW-BC in a single and binary environment in order to understand the effect of co-contamination on the adsorption process. For that batch experiments were conducted at various

laboratory conditions of pH, resident time, initial concentration, and experimental temperature; (3) assess the breakthrough effect of toluene and ethylbenzene through a fixed-bed column.

2. Material and methods

2.1. Chemical and reagent

Chemicals used in this study were purchased from Sigma Aldrich USA. The EPA 524 standards for the volatile organic compound were purchased from Sigma Aldrich (EPA VOC Mix 2, Sigma-Aldrich Co. LLC., MO, USA, Analytical standard 48,777). Purge and trap volatile grade residue-free methanol (Methanol ≥99.9%, PESTINORM 83967.290, VWR, USA) was used to prepare VOC stock solution and analytical calibration standards. Milli Q water (Thermo smart 2 ultra-pure system, Hungary) with a conductivity of 0.055 µS/cm, saturated with high purity nitrogen (grade 4.8), was utilized in all the experiments. Sodium azide (Fluka analytical Ltd, USA) was used for aqueous media preparation to avoid microbial oxidation.

2.2. Biochar production

The dried biomass of organic portion from the municipal solid waste was subjected to the pyrolysis process in the close hopper loaded without headspace (oxygen-controlled environment). The pyrolysis of municipal solid waste was done in a batch pyrolysis reactor, with ramped temperature from 30 to 450 °C for 30 min followed by a holding duration of 30 min at 450 °C (Jayawardhana et al., 2019b). The resulting biochar was immediately dropped into a water bath to down the temperature and remove ash without contacting the open atmosphere. Finally, the ash-free biochar was then air-dried and sieved through a 2 mm mesh sized sieve and stored for further batch and column experiments. Characteristics of the MSW-BC were reported in previous publications (Jayawardhana et al. 2018, 2019b, 2019d).

2.3. Adsorption experiments in a single sorbate system

All the adsorption tests were run with the control, blank samples and laboratory reagent blanks to understand the atmosphere, water environment, and MSW-BC associated behavior as a control measure. The pH edge experiment was achieved at different initial pH of 3, 5, 7, 8.3 and 9 for a spot favorable pH environment. Initially, 1 g/L of MSW-BC was hydrated under the nitrogen-purged atmosphere, which decreased atmospheric carbon dioxide and oxygen interference with the solution. The mixture of MSW-BC optimized sorbent dosage of 1 g/L obtained from previous studies to continue experiments with the toluene or ethylbenzene (50 µg/L) separately equilibrated in an incubation shaker (Cheimika RG 4110, Italy) at 100 rpm for 12 h of time. The solutions were then analyzed for the equilibrium concentration of toluene and ethylbenzene by a headspace gas chromatography-mass spectroscopy (GC-MS).

The batch kinetic experiment for the adsorption of toluene (50 µg/L) and ethylbenzene (50 µg/L) separately with 1 g/L of MSW-BC were conducted at 25 °C and pH 8. During the experiment, the resident time was varied for 0.5, 1, 2, 4, 12, 18 and 24 h. Finally, headspace was analyzed for remaining toluene and ethylbenzene concentration. The amount of adsorption (q_t , µg/g) at time t (h) was calculated by Eq. (1).

$$q_t = \frac{[C_0 - C_t]V}{M} \quad (1)$$

where C_0 and C_t the concentration of the toluene and ethylbenzene at time 0 and t (µg/L) respectively, V and M are the volumes of the solution in L and mass of MSW-BC in g.

Adsorption isotherm studies were carried out for 1 g/L of MSW-BC with different toluene and ethylbenzene concentrations (10–600 µg/L)

separately, at pH 8 and 25 °C and the resident time was kept for 12 h. Finally, the headspace was analyzed for the remaining concentration of toluene and ethylbenzene at equilibrium. The adsorption amount (q_e , $\mu\text{g/g}$) was calculated by Eq. (2).

$$q_e = \frac{[C_0 - C_e]V}{M} \quad (2)$$

where, C_0 and C_e are the initial and equilibrium toluene and ethylbenzene concentrations ($\mu\text{g/L}$), respectively, V is the solution volume (L) and M is the mass of biochar (g).

2.4. Binary adsorption system with ethylbenzene system

Batch experiments were conducted in a binary contaminant system, where 50 $\mu\text{g/L}$ of both sorbates (toluene and ethylbenzene) were added into the experiment mixture with 1 g/L MSW-BC, and the total concentration of toluene and ethylbenzene became doubled compared to that used in a single contaminant system. The solvent effect due to the methanol was balanced in both single and binary systems by keeping at 1% methanol (Bornemann et al., 2007). The toluene and ethylbenzene adsorption in a binary contaminant environment were assessed via pH edge, kinetics, and isotherm as same as described in a single contaminant system.

2.5. Thermodynamic experiments

The thermodynamic studies on the adsorption of toluene and ethylbenzene by MSW-BC in both single and binary contaminant environments were assessed at three different temperatures of 25, 35, and 45 °C. For this purpose, adsorption experiments were conducted with an initial concentration range of 30–600 $\mu\text{g/L}$ at pH 8 and the resident time was kept 12 h. The thermodynamic parameters, namely, the Gibbs free change (ΔG^0), enthalpy change (ΔH^0), and entropy change (ΔS^0), were calculated using equations (3)–(6).

$$\ln K_d = \frac{S^0}{R} - \frac{H^0}{RT} \quad (3)$$

$$\Delta G = H^0 - TS^0 \quad (4)$$

$$G = -RT \ln(K_d) \quad (5)$$

$$K_d = \frac{[C_0 - C_e]V}{C_e M} \quad (6a)$$

T represents the temperature (K), and R represents the universal gas constant (8.314 J/K/mol). The equilibrium distribution coefficient is indicated by K_d obtained from Eq. (6). The ΔH^0 and ΔS^0 were determined from the slope and intercept of plot $\ln K_d$ against $1/T$, respectively.

2.6. Column experiments and modeling

Variable bed columns were arranged by PTFE liquid chromatography column equipped with an adjustable plunger seal. The dimensions of the column were 2.5 cm, 20 cm in inner diameter and length, respectively. Column media material containing 69 g of silica sand (50 mesh size) was obtained from the Naththandiya silica sand mining area, Sri Lanka. Silica sand was used to prevent bed plugging while improving the porous structure in the column. Further, the inertness of the silica sand source material is suited for modeling and breakthrough behaviors identification (Mowla et al., 2013). The sand was washed with ultrapure water to remove impurities before packing the columns, and then it was wet packed into the column. Additional ports were arranged in the tubing line for direct sampling. Best adsorbents ratios for VOC removal were set based on the preliminary data gathered from batch isotherm studies. Inlet concentrations of toluene and ethylbenzene during the fixed bed column were maintained as 4 mg/L and were pumped from top

to bottom of the columns by a cartridge pump (Masterflex L/S, Cole-Parmer, Model 751,920, USA) at 2 mL/min flow rate. Samples were collected at the column outlet at different time intervals, while the container was cooled to 4 °C and transferred to the GCMS to measure the remaining VOCs. Three models, Thomas, Adams-Bohart, and Yoon-Nelson, were used to analyze the breakthrough curves by linear regression and predict the column performance to remove VOC from an aqueous solution.

2.7. Analysis

Toluene and ethylbenzene analysis was performed using a Gas Chromatography-Mass Spectrometry (Shimadzu QP, 2010). The GC-MS was equipped with a fused silica capillary column Rtx-624 (0.18 mm of internal diameter, 1.00 μm of film thickness, 20 m of length, Restek Scientific Inc.), a static headspace analyzer, and an autosampler (HS-20 Shimadzu, Japan). The instrument detection limit was set within the range of 0.1–0.01 $\mu\text{g/L}$. The oven temperature of the headspace analyzer was set to 70 °C to efficiently extract BTEX while keeping the thermal degradation and controlling water vapor pressure, optimum recovery of analyte achieved (Flórez Menéndez et al., 2000; Jayawardhana et al., 2019b; Soria et al., 2015). The GC was programmed for temperature increased from 35 °C to 230 °C at 20 °C/min of heating rate, allowing 14 min for optimum separation. The carrier gas was high purity He (99.9996%) with a 24.7 mL/min flow rate (Shimadzu 2013).

3. Results and discussion

3.1. Single sorbate experiments

3.1.1. Influence of solution pH

All the control and laboratory reagent blanks express below LOD for all the EPA 524 protocol elements with a favorable experimental design condition. The experimental spike control of the sample range (10–600 $\mu\text{g/L}$) was in agreement with the validated EPA 524; no abiotic degradation was observed for any samples and acceptable recovery observed for all. The variation in the adsorption amount of BTEX in a mono-sorbate system by MSW-BC as a pH function is shown in Fig. 1(A). The adsorption of ethylbenzene moderately depends on the pH and a high adsorbed amount (45.82 $\mu\text{g/g}$) was recorded at a basic pH of 9. The adsorption of toluene onto the MSW-BC showed wave-like changes with the function of pH and the highest adsorption (44.87 $\mu\text{g/g}$) was noted at a pH of 8.3. Then, the adsorbed amount of toluene and ethylbenzene was fallen between 41 and 42 $\mu\text{g/g}$ with decreasing pH up to 3. The slight differences in the adsorption trends result in the non-electrostatic attraction between the MSW-BC and toluene or ethylbenzene (Keerthanan et al., 2020a). The same adsorption phenomenon described by Nourmoradi et al. (2013) has further been described with π - π stacking in adsorption of aromatics by carbon-based materials (Bianco et al., 2021; Chin et al., 2007). Besides, both toluene and ethylbenzene at elevated pH in an agreement of higher adsorption reveal by Carvalho et al. (2012) for organically with the presence of hydroxyl group that can be attributed slight variation of adsorption over pH.

3.1.2. Adsorption kinetic and modeling

The kinetic trends of toluene and ethylbenzene in the single contaminant system as a function of time are presented in Fig. 2(A) and (B). The adsorption amounts of toluene and ethylbenzene were speedily boosted within the first 5 h and later, adsorption affinity was approached to a constant amount. This observation might be due to a high number of active sites in MSW-BC than the number of toluene or ethylbenzene at the beginning, which leads to boost the adsorption, and later, once the active sites on MSW-BC became occupied by toluene or ethylbenzene with mixing time, the adsorption process reached equilibrium. The adsorption behavior of sorbent proved with other studies evident for vacant site favorability for both alkyl benzene

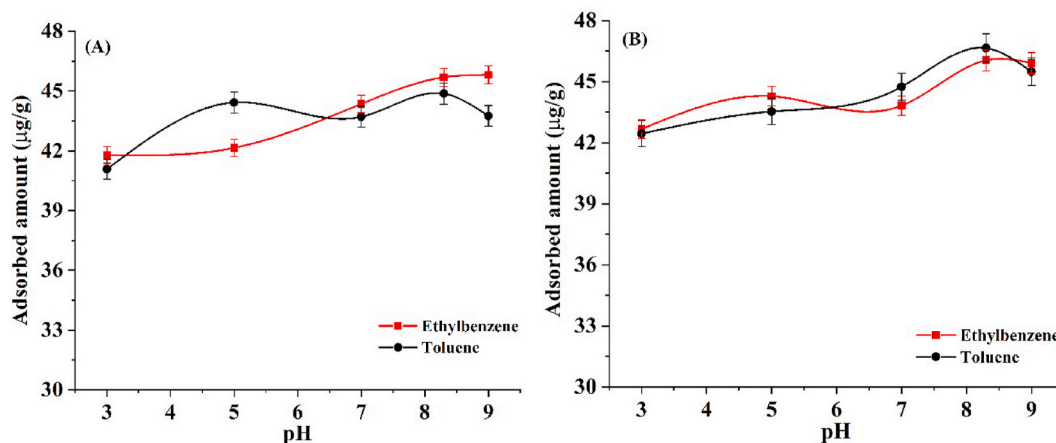


Fig. 1. The adsorption variation of toluene and ethylbenzene in: (A) single system and (B) binary system, as a function of pH at 25 °C.

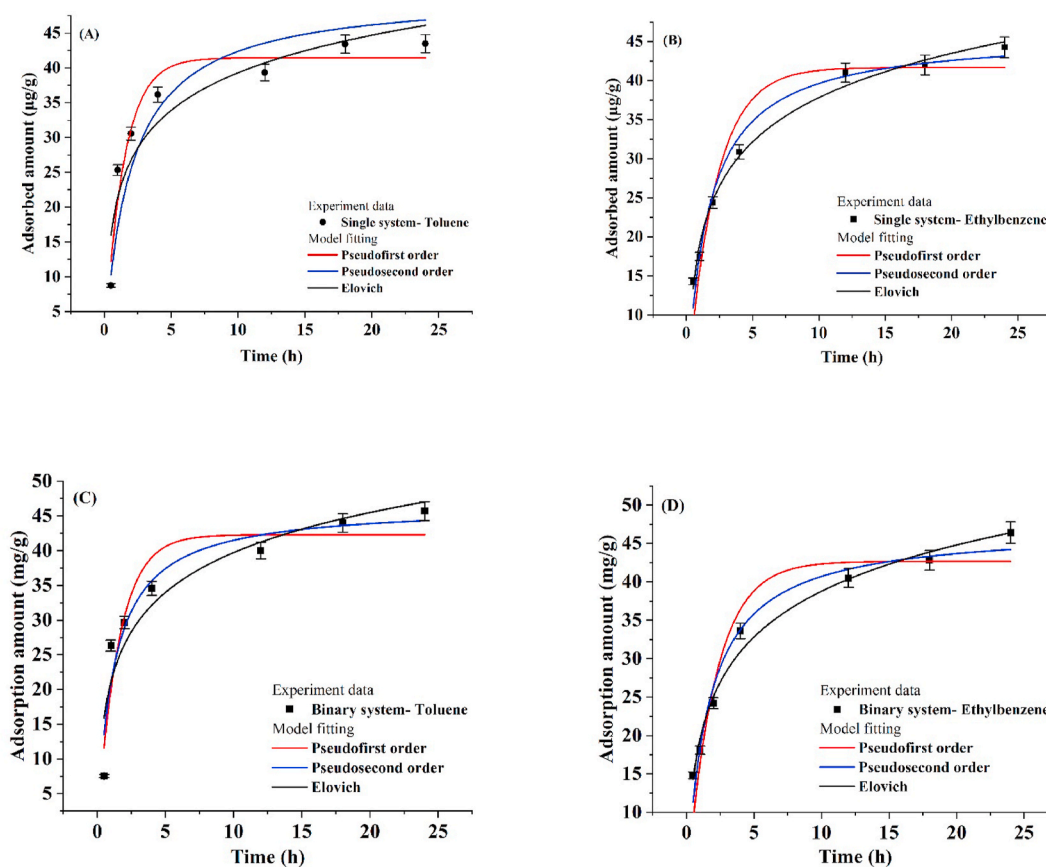


Fig. 2. The kinetic fitted models of: (A) toluene and (B) ethylbenzene in single contaminant system, and (C) toluene and (D) ethylbenzene in binary contaminant system.

simultaneously, which can be attributed to reducing the active sites by approaching the saturation state (Rajarithnam et al., 2020).

The kinetic data were simulated with pseudo-first-order, pseudo-second-order, and Elovich kinetic models. The predicted kinetic parameters are tabulated in Table 1 and the fitting plots are exhibited in Fig. 2. The fitting models were fallen in the order of Elovich > Pseudo second-order > Pseudo-first-order for the ethylbenzene adsorption as the correlation coefficient (R^2) was decreased in the same order from 0.99 to 0.93. Meanwhile, model fitting for toluene in a single contaminant system has been obtained in the order of pseudo-second-order > pseudo-first-order > Elovich based on R^2 decreased from 0.94 to 0.88

(Table 1). The maximum adsorption capacity predicted from the pseudo-second-order of ethylbenzene and toluene were 45.9 and 45.3 $\mu\text{g/L}$, respectively, and this predicted adsorption capacities were much closer to the experimental values (46.4 and 43.5 $\mu\text{g/L}$, respectively). The best fitted kinetic model of pseudo-second-order suggests that the adsorption of toluene and ethylbenzene onto MSW-BC were mainly enforced by monolayer adsorption through the electron exchange process in a single contaminant system. The Elovich model suggests the nature of the adsorption process with chemical forces' involvement at the heterogeneous surface. However, Elovich does not suggest any particular mechanism between adsorbate and adsorbent (de la Luz-Asunción et al.,

Table 1

Kinetics properties of the ethylbenzene, toluene single and binary system (control condition 50 µg/L, 24 h, 25 °C).

Kinetics	Parameter	Single		Binary	
		Toluene	Ethylbenzene	Toluene	Ethylbenzene
Pseudo second order	Q_{max}	45.3	45.9	46.5	47.1
	K_2	0.020	0.014	0.018	0.013
	R^2	0.944	0.979	0.929	0.975
	χ^2	40	11	15	5
Elovich	A	121.73	83.92	100.1	87.46
	B	0.12	0.12	0.12	0.11
	R^2	0.88	0.991	0.897	0.987
	χ^2	68	3	23	2
Pseudo first order	q_{max}	41.4	41.6	42.2	42.6
	K_1	0.69	0.46	0.64	0.48
	R^2	0.942	0.930	0.907	0.929
	χ^2	28	31	19	13

2020). The most fitted kinetic models suggest that the toluene and ethylbenzene in a single system interact with MSW-BC via an electron exchange process such as specific interaction (Hydrogen- π and cation- π electron exchange process) (Bianco et al., 2021). The Daifullah and Giris (2003) reported the electron exchange mechanism between BTEX and activated carbon.

3.1.3. Adsorption isotherm and modeling

The isotherm regression of Langmuir, Freundlich, and Hill models was fitted with the isotherm results and the predicted parameters along with R^2 are charted in Table 2 and the fitted models are shown in Figs. 3 and 4. The Langmuir and Hill models were well-fitted with isotherm results, followed by the Freundlich model as based on the R^2 (at > 95%) (Table 2). The Langmuir model hypothesized that a monolayer saturation occurs at homogeneously distributed active sites by energy (Shirani et al., 2020). The saturation capacities of toluene predicted by the Langmuir model were 1090, 879, and 850 µg/g at 25, 35, and 45 °C, respectively. Meanwhile, the saturation capacities were 619, 650, and 655 µg/g for ethylbenzene in a single contaminant system.

The Hill model also showed an identical fitting as the Langmuir model with the isotherm results (Table 2). The Hill model postulated to cooperative adsorption of toluene or ethylbenzene occurs onto the homogeneously distributed active sites on the surface of the MSW-BC, and the binding energy of an active site influenced by the binding energy of other active sites on the homogeneous surface (Atugoda et al., 2020; Sivarajasekar and Baskar 2019). Generally, the nature of cooperative adsorption was predicted by the Hill cooperativity coefficient (n_H). When $n_H > 1$, this postulate positive cooperativity in binding. When $n_H < 1$, this assumes negative cooperativity in binding. When $n_H = 1$, this indicates non-cooperative binding between adsorbate and adsorbent

(Atugoda et al., 2020). For the toluene adsorption in a single contaminant system, the n_H was higher than unity at 25 °C indicates, the positive cooperativity, which means the adsorption of toluene at a particular active site in MSW-BC, enhanced by another active site. However, the adsorption became non-cooperative at 35 and 45 °C since the $n_H \approx 1$. Similarly, the adsorption of ethylbenzene also showed non-cooperativity adsorption at 25, 35, and 45 °C since the $n_H \approx 1$ (Table 2). Further, Hill's constant (KD) positive value indicates that the electrostatic and hydrophobic interaction was the dominant attraction employed between the BETX compound and MSW-BC (Atugoda et al., 2020). The modified Boehm data express the total acidic, basic, carboxylic, lactone, and phenol group in the MSW-BC, which phenolic can enhance the electrostatic interaction (Jayawardhana et al., 2019a; Zhang et al., 2018). All in all, the predicted isotherm models portray the non-cooperative toluene or ethylbenzene adsorption that took place at the homogeneous surface of MSW-BC in a single contaminant environment.

3.2. Competitive adsorption behavior of ethylbenzene and toluene

The competitive adsorption process can depend on several phenomena and constituents. In alkyl benzene, polarity, molecular size and molecular velocity can affect the collision and competitive adsorption. The environment (pH, solubility, temperature, and surface chemistry) may influence or hinder the reaction according to the reaction kinetics and the toluene and ethylbenzene adsorption thermodynamics.

3.2.1. pH dependency of the binary ethylbenzene and toluene

The adsorption of toluene and ethylbenzene in the binary contaminant environment was slightly dependent on pH (Fig. 1 (B)). The highest saturation capacity of 46.65 and 46 µg/g for toluene and ethylbenzene, respectively, were observed at a pH of 8.3, and the saturation capacities were decreased with dropping pH toward acidic pH. A mild enhancement in toluene and ethylbenzene adsorption is observed in the binary system compared to a single contaminant system. The literature agreement with sorbent-sorbate interaction in binary system possible tendency for slight decrease with lower pH by hindering active sites in MSW-BC via making hydrogen bonding (Carvalho et al., 2012). However, the total saturation capacity of MSW-BC for toluene and ethylbenzene was doubled in the binary system than those in a single system. This observation illustrated the co-contamination effect; adsorption of one contaminant enhances by the presence of others. Hence, the pH_{PZC} of the MSW-BC was 6.7, which indicates the MSW-BC surface dominated by the negative charge at the higher pH. Further, ethylbenzene and toluene dominantly represent in the molecular form at a pH of 3–9 (Wibowo et al., 2007). The interaction between toluene and ethylbenzene and MSW-BC may have occurred via the hydrophobic and anti π bonding.

Table 2

Isotherm parameters for toluene, Ethylbenzene adsorption onto MSW-BC under single and binary experimental setup (pH 8.3).

Isotherm	Parameter	Single system						Binary system					
		Toluene			Ethylbenzene			Toluene			Ethylbenzene		
		25 °C	35 °C	45 °C	25 °C	35 °C	45 °C	25 °C	35 °C	45 °C	25 °C	35 °C	45 °C
Langmuir	q_{max}	1090	879	850	619	650	655	1183	887	834	998	1273	993
	K_L	0.007	0.01	0.01	0.02	0.03	0.04	0.006	0.01	0.01	0.01	0.008	0.01
	R^2	0.972	0.997	0.993	0.990	0.985	0.990	0.999	0.990	0.989	0.984	0.982	0.986
	χ^2	32	25	17	299	481	343	19	359	385	14	13	26
Freundlich	K_F	–	–	–	36.5	41.2	53.5	14.8	28.3	33.1	23.3	20.3	30.6
	N	–	–	–	1.82	1.81	1.90	1.32	1.57	1.62	1.42	1.33	1.50
	R^2	–	–	–	0.960	0.954	0.945	0.995	0.988	0.997	0.987	0.989	0.995
	χ^2	–	–	–	1182	1487	1889	175	410	113	21	22	7
Hill	K_D	0.02	0.01	0.01	0.03	0.03	0.05	0.007	0.005	0.001	0.002	0.005	0.003
	n_H	1.76	0.95	0.98	1.04	1.05	1.14	1.01	0.82	0.69	0.78	0.90	0.78
	q_{SH}	578	954	874	594	617	593	1130	1319	2460	2670	1608	1926
	R^2	0.992	0.997	0.993	0.990	0.985	0.992	0.999	0.992	0.997	0.987	0.985	0.994
	χ^2	23	10	8	331	531	317	23	346	105	17	16	7

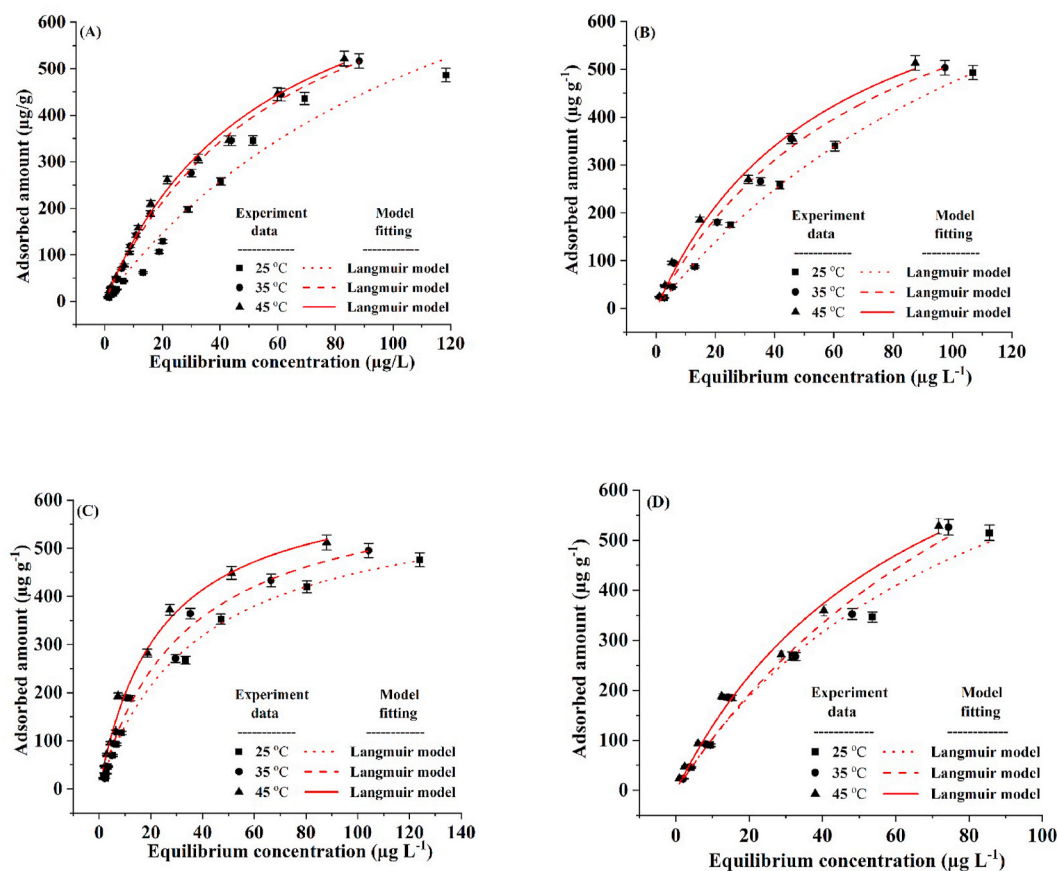


Fig. 3. The Langmuir isotherm fitted of toluene in (A) single contaminant system and (B) binary contaminant system, and ethylbenzene in (C) single contaminant system and (D) binary contaminant system, at 25, 35, and 45 °C.

3.2.2. Kinetics behavior of ethylbenzene with the competition of toluene

The kinetic results in the binary system, along with the fitted non-linear models of pseudo-second-order, Elovich, and pseudo-first-order, are provided in Fig. 2(C) and (D) and the predicted parameters are tabulated in Table 1. The most fitted models for toluene adsorption in the binary contaminant system were dropped in pseudo-second-order > pseudo-first-order > Elovich, whereas for ethylbenzene, the order was Elovich > pseudo-second-order > pseudo-first-order. The adsorption capacities of toluene and ethylbenzene predicted from the pseudo-second-order were increased slightly in the binary system compared to the single system. The current preference order of toluene and ethylbenzene ($\log K_{ow}$ 2.73, 3.15) can be attributed to the physicochemical properties of the compounds, hydrophobicity (Carvalho et al., 2012; Lima et al., 2017). However, the pseudo-second-order rate constants decreased in the binary system, indicating greater competition between the toluene and ethylbenzene molecules during the adsorption onto the MSW-BC. The pseudo-second-order model assumes that the rate-limiting step occurs via the electron exchange between adsorbate and adsorbent (Noufel et al., 2020). The initial rate constant (α) predicted from the Elovich model decreased for toluene; meanwhile, α increased for ethylbenzene in the binary system compared to a single system. This trend might be due to the co-contaminant effect resulted from the competition between toluene and ethylbenzene in the adsorption process. Moreover, the desorption constant (β) predicted from the Elovich model was less and constant for toluene adsorption in the binary system; simultaneously, β decreased for ethylbenzene, compare to a single system (Table 1). This observation demonstrated no extend of surface coverage during the adsorption process and this revealed the strong interaction between toluene and ethylbenzene and MSW-BC.

3.2.3. Adsorption isotherms of ethylbenzene at the presence of toluene

In a binary contaminant system, simultaneous adsorption of toluene and ethylbenzene takes place onto the MSW-BC under the influence of each other. The competition adsorption of toluene and ethylbenzene in the binary mixture is described through the non-linear regression of Langmuir, Freundlich, and Hill models. All three models were fitted to the isotherm results as the correlation coefficient (R^2) closer to unity. The Langmuir model suggested that monolayer adsorption occurs at the homogeneous surface (Noufel et al., 2020). Compared to the single contaminant system, the Langmuir adsorption capacity (Q_{max}) values slightly increased to toluene adsorption, whereas significantly increased to ethylbenzene, indicates the adsorption of toluene or ethylbenzene by the MSW-BC enhanced by the presence of ethylbenzene or toluene, respectively in the binary system. The Freundlich model assumes that the multilayer adsorption occurs at the heterogeneous surface (Keerthanan et al., 2020b). The Freundlich adsorption intensity ($1/N$) values were below the unity, indicates the favorability of toluene and ethylbenzene adsorption by MSW-BC. The Hill maximum saturation capacities were significantly increased for both toluene and ethylbenzene in a binary contaminant system.

Moreover, the Hill cooperativity coefficients (n_H) for toluene and ethylbenzene in the binary system were below than one at three operating temperature, except the n_H for toluene adsorption at 25 °C (Table 2), indicates the occurrence of negative cooperativity adsorption between toluene and ethylbenzene molecules, and MSW-BC. Overall, the isotherm models suggest a complicated adsorption mechanism between toluene and ethylbenzene molecules and MSW-BC. The hydrophobic interaction can be a suggested mechanism in this adsorption process. This interaction probably explains by the octanol-water partition coefficient ($\log K_{ow}$) of toluene and ethylbenzene. The $\log K_{ow}$ of

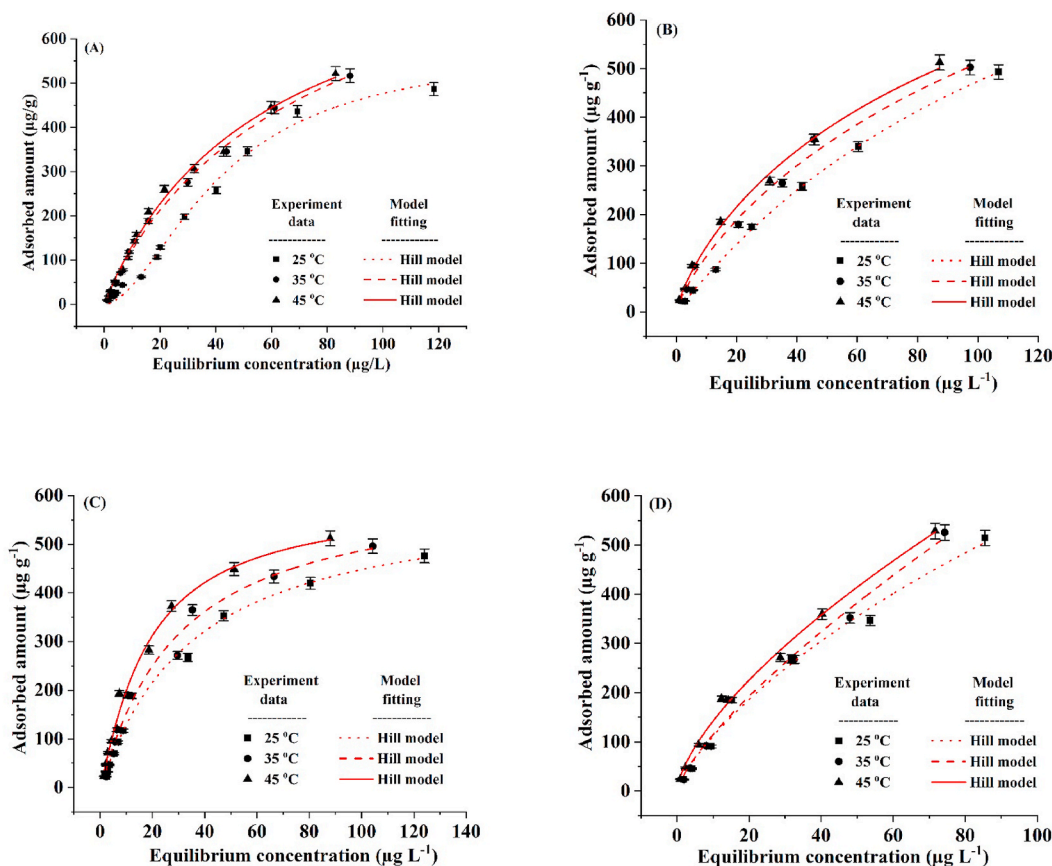


Fig. 4. The Hill isotherm fitted of toluene in (A) single contaminant system and (B) binary contaminant system, and ethylbenzene in (C) single contaminant system and (D) binary contaminant system, at 25, 35, and 45 °C.

toluene and ethylbenzene was 2.73 and 3.15, respectively. This distinction in log Kow determines the highest affinity to ethylbenzene toward the surface of MSW-BC. Moreover, electrostatic, π - π interaction and n- π attraction, van der Waals interaction, and specific interaction (Hydrogen- π and cation- π interactions) also possible interaction involved in the adsorption of toluene and ethylbenzene onto MSW-BC.

3.2.4. Effect of co-contaminants on the adsorption

The simultaneous adsorption of a contaminant in co-contaminants is another crucial aspect to understand the contaminant behaviors in a binary system. For this purpose, the ratio of adsorption capacity (R_q) was estimated using equation (6) (Jiang et al., 2018).

$$R_q = \frac{q_{b,i}}{q_{m,i}} \quad (6b)$$

where, $q_{b,i}$ and $q_{m,i}$ are termed as adsorption capacity of contaminant i (toluene and ethylbenzene) in a binary and single contaminant system, respectively. When $R_q > 1$, the adsorption of contaminant i boosted owing in the presence of co-contaminants (synergism). When $R_q < 1$, the adsorption of contaminant i discouraged due to the presence of co-contaminants (antagonism). When $R_q = 1$, the adsorption of contaminant i is not influenced by the presence of co-contaminants (non-interaction). The results of R_q as a function of initial concentration was plotted in Fig. 6. A synergistic interaction ($R_q > 1$) was observed on the adsorption of toluene in the existence of ethylbenzene. When the initial concentration increased, the R_q value increased at all the experimental temperatures for both toluene and ethylbenzene. Moreover, the influence of toluene in the adsorption of ethylbenzene was observed above the 50 $\mu\text{g/g}$ of initial concentration. Below 50 $\mu\text{g/g}$, the R_q is closer to 1, indicating that the toluene did not influence the ethylbenzene

adsorption in the binary system. All in all, the synergistic effect could be demonstrated where the MSW-BC has shown different adsorption affinities for toluene and ethylbenzene at lower initial concentrations and which led to interaction via chemisorption (monolayer). When the initial concentration increased, the adsorption of toluene and ethylbenzene leads to influence via the physisorption (multilayer).

3.3. FTIR analysis

The FTIR spectra, as shown in Fig. 5, the stretching oscillation at 3426 cm^{-1} can be described as the presence of -OH, belongs to phenolic or carboxylic acid on the surface of pristine MSW-BC. The peaks observed at 2923, 1638, and 1029 cm^{-1} demonstrated the occurrence of aliphatic C-H, C=O, and C-O groups on the MSW-BC surface, respectively (Fig. 5 (A)) (Ashiq et al., 2019b; Jayawardhana et al., 2019d). The FTIR spectra of toluene and/or ethylbenzene incorporated MSW-BC provided in Fig. 5(B)–(D), where the observed peaks at 3150–3250, 2150–1950, 1614, and 615 cm^{-1} correspond to aromatic C-H stretching, combination and overtone bands for aromatic rings, aromatic C=C stretching, and out of plan C-H bending (Pavia et al., 2008), respectively, indicating the successful incorporation of toluene and ethylbenzene with MSW-BC. A sustainable option of the immobilization of organic compounds in the biochar has been proven for long term stability with different environmental conditions along the bonded surfaces. It can be followed for the same in MSW-BC for organic substances via the adsorption process.

3.4. The thermodynamic aspect of competitive sorption system ethylbenzene and toluene

Thermodynamic results express the spontaneous and non-

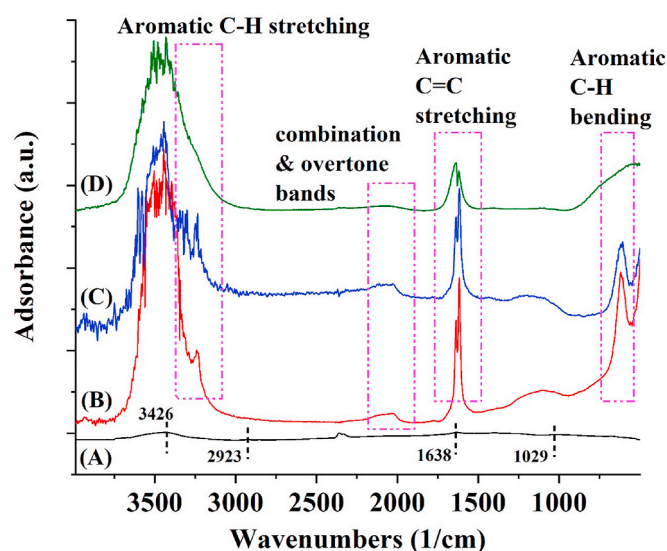


Fig. 5. The FTIR spectroscopy of (A) bare MSW-BC, (B) toluene adsorbed MSW-BC, (C) ethylbenzene adsorbed MSW-BC, and (D) toluene and ethylbenzene adsorbed MSW-BC in binary system.

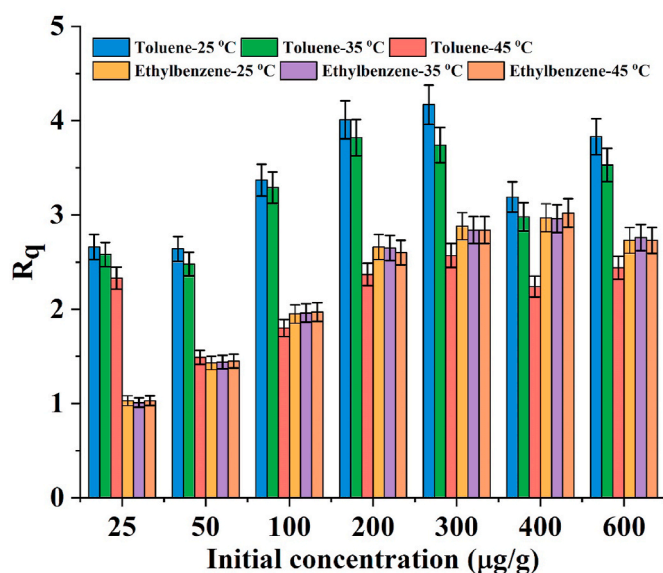


Fig. 6. The effect of co-contaminant in term of R_q as the function of initial concentration.

spontaneous reaction behavior of possible reaction occurrence with the sorbent-sorbate interaction under the specific temperature (Hercigonja et al., 2012). The calculated thermodynamics parameters are given in Table 3 for toluene and ethylbenzene in a single and binary system. The

Table 3

Thermodynamic properties of the ethylbenzene and toluene under the single and binary experimental setup.

Parameter	Single		Binary	
	Toluene	Ethylbenzene	Toluene	Ethylbenzene
ΔH^0 (kJ/mol)	-16.82	-16.41	-9.49	-8.06
ΔS^0 (J/mol/K)	68.60	66.28	44.52	42.12
ΔG^0 (kJ/mol)				
25 °C	-37.26	-36.16	-22.75	-20.61
35 °C	-37.95	-36.83	-23.20	-21.03
45 °C	-38.64	-37.49	-23.64	-21.45

value of ΔG^0 expresses the nature of the reaction, either spontaneous or non-spontaneous. From the results of this study, it can be seen that all the systems obey the rule of negative value in favor of the adsorption phenomenon with spontaneous nature (Table 3). The ΔG^0 of all single and binary systems negatively increased with the increasing temperature, indicating much favorability at higher temperatures with molecular velocity and the higher driving force. The positive ΔS^0 value indicates the randomness adsorption at the solid-liquid interface, which occurs due to the displacement of water molecules, result in uptake of toluene and ethylbenzene by MSW-BC (Rincón-Silva et al., 2015). Further, the ΔS^0 decreased for toluene and ethylbenzene adsorption in the binary system, compared to a single system, manifests the randomness adsorption decreased in the binary system, indicating the influence of ethylbenzene or toluene in the adsorption of toluene and ethylbenzene. The negative ΔH^0 pinpoints that the adsorption of toluene and ethylbenzene by MSW-BC is an exothermic reaction. The ΔH^0 value obtained by toluene and ethylbenzene adsorption by MSW-BC found to be lower than 40 kJ/mol, indicates the involvement of physical forces in the adsorption process (Inyınbor et al., 2016).

3.5. Column breakthrough analysis

The breakthrough curve obtained for the adsorption of toluene and ethylbenzene at various conditions is shown in Fig. 7 (A). The toluene shows less breakthrough time than ethylbenzene at the same operational conditions due to the low affinity of toluene with solid-phase compared to ethylbenzene. The obtained fixed column data were utilized with Yoon-Nelson, Thomas, and Adams-Bohart models. The applicability of linear models was determined with the correlation coefficient (R^2) and Pearson's coefficient (r), tabulated in Table 4. For the toluene, the Adams-Bohart was fitted with experiment results, followed by Yoon-Nelson and Thomas models, while the Yoon-Nelson and Thomas were compatible-models followed by Adams-Bohart in the ethylbenzene retention on fixed column bed, based on R^2 .

The linear regression plots of toluene and ethylbenzene adsorption onto the bed column are shown in Fig. 7 (B) and the predicted parameters are provided in Table 4. The Yoon-Nelson model was positively correlated with the experimental results based on Pearson's correlation coefficient (Table 4). The Yoon-Nelson rate constant (K_{YN}) and Yoon-Nelson adsorption capacity (q_{YN}) for the adsorption of ethylbenzene was relatively higher than those of toluene. The higher K_{YN} described that the adsorption reached saturation speedily due to the high mass loaded into the fixed bed (Ang et al., 2020). The time taken to reach a 50% breakthrough (τ) of toluene and ethylbenzene predicted by the Yoon-Nelson model was good agreement (Table 4) with experimentally calculated values (Fig. 7 (A)).

Thomas model rate constant (k_{TH}) and the maximum adsorption capacity (q_{TH}) were determined through the linear regression plot shown in Fig. 7 (C) and the values are provided in Table 4. Thomas model exposed a negative correlation with experimental results in Pearson's r (Table 4). The value of k_{TH} for the adsorption of ethylbenzene was 2-fold higher than those for toluene. Similarly, the q_{TH} was also significantly higher for ethylbenzene than toluene adsorption. The predicted value was in good cooperation with the experimental results. Hence, the Thomas model is desirable for the adsorption in which the internal and external diffusion was not a limiting step (Chen et al., 2012).

The Adams-Bohart model is accurate under conditions where the sorption isotherm is extremely favorable (Edathil et al., 2020). It assumes that the equilibrium is not rapid; therefore, the adsorption rate is proportional to the adsorption amount being adsorbed onto fixed bed adsorbent (Li et al., 2020). The Adams-Bohart model positively correlates with the experimental results as per Pearson's r (Table 4). The model predicted values of adsorption capacity per unit volume of the bed column (N_0) and Adams-Bohart rate constant (K_{AB}) on the adsorption of toluene and ethylbenzene are presented in Table 4 and the model

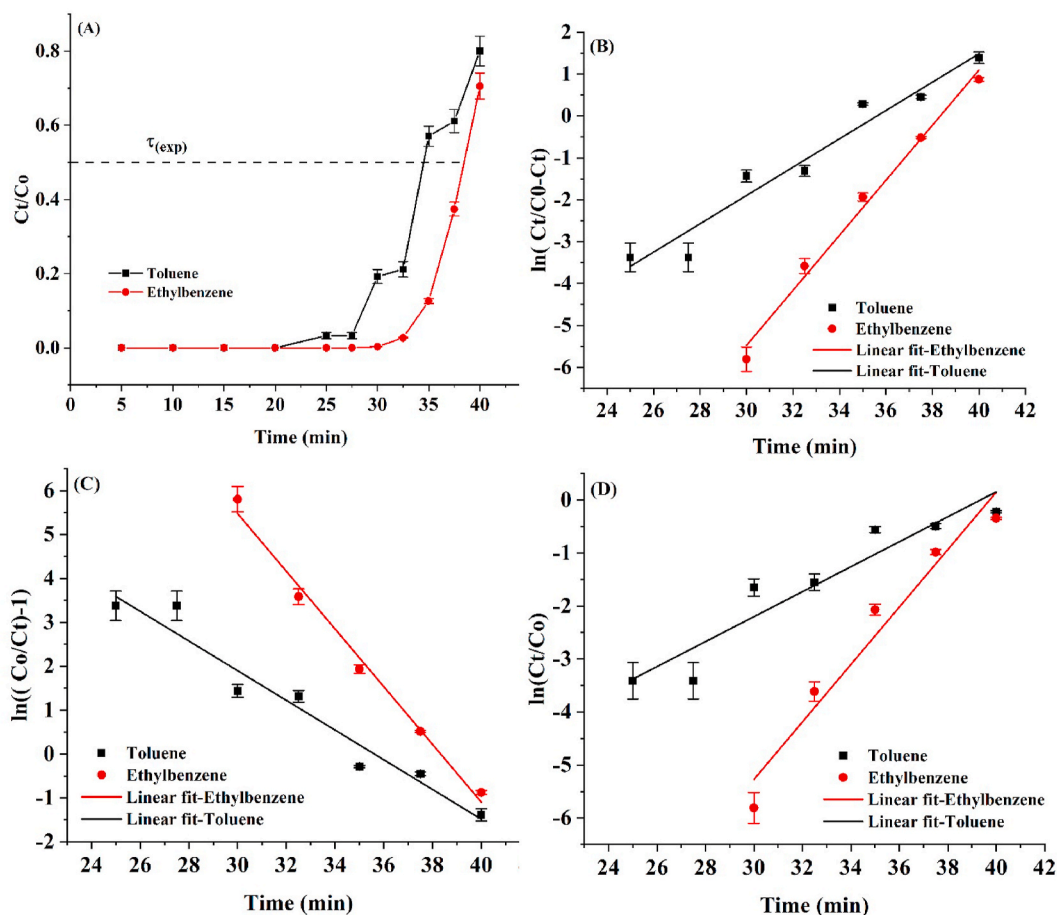


Fig. 7. Breakthrough curve (A), Yoon-Nelson (B), Thomas (C), and Adams-Bohart (D) models for the adsorption of toluene and ethylbenzene at various conditions of 4 mg/L influent concentration, 2 mL/min flow rate, and 0.25% MSW-BC.

Table 4

The predicted parameters by the fixed bed column for the adsorption of toluene and ethylbenzene.

Models	Parameters	Toluene	Ethylbenzene	
Yoon-Nelson (Ang et al., 2020; Singh et al., 2017)	$\ln\left(\frac{C}{C_0 - C}\right) =$	K_{YN} (1/min)	0.3382	0.6571
	$K_{YN}t - \tau K_{YN}$	τ (min)	35.6172	38.33725
	$q_{YN} = \frac{\tau C_0 Q}{1000M}$	q_{YN} ($\mu\text{g/g}$)	4.130	4.445
		R^2	0.94216	0.98606
		Pearson's r	0.9756	0.99476
		SS	1.01	0.29
Thomas (Ang et al., 2020)	$\ln\left(\frac{C_0}{C} - 1\right) =$	k_{TH} (ml/ μg min)	0.084543	0.164275
	$\frac{k_{TH} q_{TH} M}{Q} - k_{TH} C_0 t$	q_{TH} ($\mu\text{g/g}$)	4129.531	4444.899
		R^2	0.94216	0.98606
		Pearson's r	-0.9756	-0.99476
		SS	1.01	0.29
Adams-Bohart (Li et al., 2020)	$\ln\left(\frac{C}{C_0}\right) =$	K_{AB} (ml/ μg min)	0.05888	0.135463
	$K_{AB} C_0 t - \frac{K_{AB} N_0 z}{U_0}$	N_0 ($\mu\text{g/L}$)	3206.777	3237.735
		R^2	0.88256	0.9364
		Pearson's r	0.94981	0.97586
		SS	1.05	0.92

SS: Sum of residual squared.

plot is shown in Fig. 7 (D). The rate constant was 0.135 mL/ μg min for the adsorption of ethylbenzene, whereas 0.059 mL/ μg min for the toluene adsorption. Although the rate constant for both adsorbates varied, the adsorption capacity was almost equal (the ratio of N_0 –

toluene to N_0 – ethylbenzene is 0.99).

Overall, the kinetic rate constants predicted by all three models for the adsorption of ethylbenzene on to the fixed bed column were significantly higher than those for toluene adsorption, portrayed smaller mass-transfer resistance of ethylbenzene and also seen in the sharper breakthrough curve shown in Fig. 7 (Ang et al., 2020).

3.6. Mechanistic determination of toluene and ethylbenzene adsorption

The possible mechanism through which the toluene and ethylbenzene interact with MSW-BC was elaborated based on the adsorption studies, bed column experiment, and FTIR analysis. The predicted data models suggested that a complicated adsorption mechanism driving via hydrophobic interaction, π - π attraction, n- π interaction and anti- π -orbital interaction existed between the MSW-BC, and toluene and ethylbenzene (Fig. 8). The abundance of hydrophobic sites on the MSW-BC makes a dominant interaction on the toluene and ethylbenzene adsorption since those adsorbents are non-polar organic substances. The MSW-BC exhibits a graphene-like nature with π electron cloud over the graphene plane, and this π electron cloud can interact with the π electron cloud of the benzene ring of toluene and ethylbenzene via a π - π interaction. The formation of additional aromatic C=C stretching bands at 1617/cm in the toluene or ethylbenzene adsorbed MSW-BC, which indicate the existence of π - π interaction (Tran et al., 2017). Moreover, n- π interaction is another possible mechanism between adsorbent and adsorbate (Keerthanan et al., 2020b). Here the oxygen and/or nitrogen on the MSW-BC surface acts as a lone pair electron donor, while the benzene ring of toluene and ethylbenzene acts as an electron acceptor, and which facilitates the existence of n- π interaction between MSW-BC,

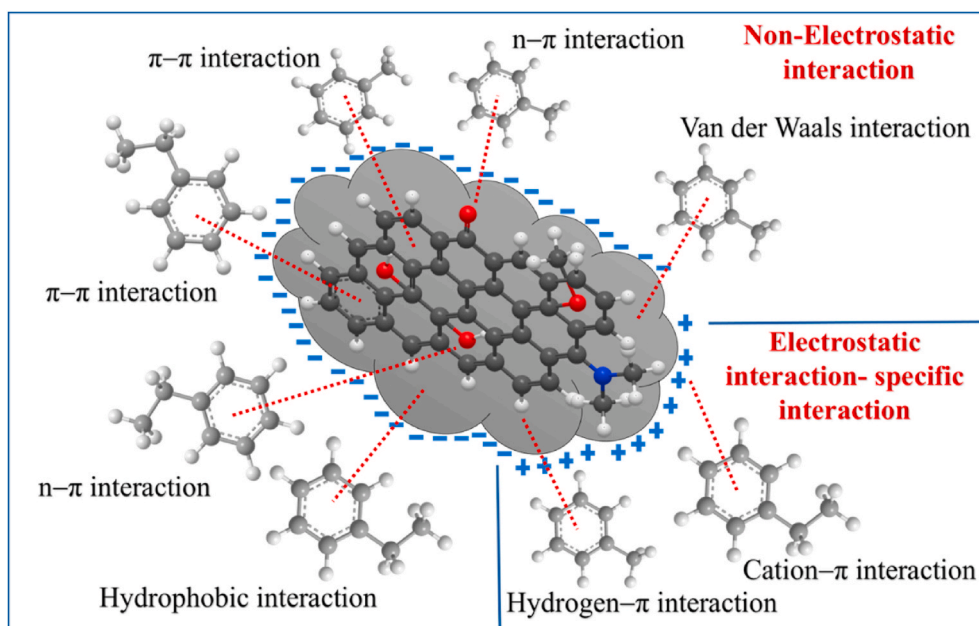


Fig. 8. The possible mechanistic ways of adsorption toluene and ethylbenzene.

and toluene and ethylbenzene. Process of adsorption, specific interaction of cation- π and hydrogen- π can occur while cationic functional groups (e.g. Na^+ , K^+). Furthermore, the presence of functional groups in the biochar at 450 °C (i.e. $-\text{COOH}$, $-\text{OH}$, and $-\text{NH}_2$) can be supported by the adsorption process (Bianco et al., 2021). The FTIR analysis shows pointedly up-shift and broadening of C–O stretching band of MSW-BC originally at 1029/cm, indicative of the occurrence of n- π interaction between MSW-BC, and toluene and/or ethylbenzene. Further, another weak interaction, for instance, van der Waals interaction, also possibly enhanced the adsorption of toluene and ethylbenzene onto MSW-BC.

4. Techno-economic analysis

The techno-economic cost was estimated from the previous studies of Hamdy et al. (2019) and Ramanayaka et al. (2020). The production cost and capital cost were estimated for the pyrolysis of 1 kg of solid waste feedstock. The production cost and capital cost were estimated in different cases, including equipment cost, utility cost, maintenance cost, and fixed and extra cost. The waste feedstock available for free since the dumping site received about 130 tons of municipal solid waste per day (Wijesekara et al., 2015). The equipment cost was examined at \$0.50 per kilogram of waste. The installation and technical costs were estimated at 20% of the cost of equipment. The utility cost, including the power source, water, and drying and sieving cost, was quantified as \$0.088/kg. The total production cost (TPC) of \$0.688 was evaluated for the pyrolysis of 1 kg of feedstock.

The estimated cost of all involved assets during the pyrolysis of municipal solid waste was tabulated in Table 5. Besides the TPC, the total capital cost was approximated at \$0.085, which included maintenance, laborer, fixed assets cost. The production of MSW-BC is economically feasible since the feedstock is available for free, and once the equipment is established, it approximately costs \$0.173 (equal to about Rs.32 Sri Lankan rupees). The MSW-BC is an inexpensive adsorbent than the activated carbon (Silva et al., 2020). A study of Lima et al. (2008) reported the production cost of activated carbon as \$1.44/kg. The modification of MSW-BC was applied with the removal perspective from the media after the saturation with the recent attention of magnetization. The respective mechanisms of magnetization significantly reduce the adsorption capacity and the cost of unit remediation requirement increase with magnetization cost and more consumption.

Table 5

The estimated cost for the pyrolysis of 1 kg of municipal solid waste.

Items	Estimated cost
Production cost	
Equipment	\$0.50/kg
Installation and technical cost	\$0.10/kg
Power source (18000 kJ)	\$0.08/kg
Water	\$0.001/kg
Drying and sieving	\$0.007/kg
Feed stock	\$0.00/kg
Total production cost	\$0.688/kg
Capital cost	
Maintenance cost	\$0.01/kg
Laborer cost	\$0.05/kg
Fixed assets cost	\$0.01/kg
Extra cost	\$0.015/kg
Total capital cost	\$0.085/kg

Furthermore, the oleic modification was encouraged to remove the environment after the saturation by supporting hydrophobicity and adsorption reduction observed for the experiment. Hence, a significant increase of MSW-BC consumption for unit amount of contaminant remediation while increasing additional production cost, bare MSW-BC, serves a much cost-effective option.

5. Conclusion

The current study goal was to produce low-cost adsorbent from municipal solid waste to remediate BTEX compounds from the aqueous media in a single and binary contaminant system. In the single contaminant system, the MSW-BC showed a similar sorption capacity for both toluene and ethylbenzene. In the binary system, the toluene and ethylbenzene exhibited little enhancement in adsorption capacity. The synergism effect was observed during the parallel adsorption of toluene and ethylbenzene onto the MSW-BC at all three experimental temperatures; co-contaminant presence enhanced the adsorption toluene and ethylbenzene to each other. The thermodynamic experiment suggested that exothermic adsorption occurred via the physical-based attraction. The breakthrough models of Yoon-Nelson, Thomas, and Adams-Bohart were successfully linearly correlated with the experimental results along with a fair agreement. The predicted kinetic rate constants of all

three models were relatively higher for ethylbenzene adsorption, suggesting a smaller mass transfer resistance through the fixed bed column. The future direction of desorption studies of BTEX in the MSW-BC with different environmental condition evaluation will support the exact leachability in the sorbent. Further studies need to address MSW-BC modification while keeping adsorption properties suitable for a sustainable removal approach after the treatment with regeneration capability.

Author contribution

Yohan Jayawardhana: Experimentation, Data interpretation, Data validation, Writing the first draft. S. Keerthan: Data validation, Writing the first draft, Reviewing and editing. Shi Shiung Lam: Writing-reviewing and editing. Meththika Vithanage: Conceptualization, Supervision, Project administration, Funding acquisition, Writing-reviewing and editing

Declaration of competing interest

The authors declare that they have no known competing financial interests or personal relationships that could have appeared to influence the work reported in this paper.

Acknowledgments

Authors hereby acknowledge National Research Council Target Oriented Grant 18–021, Sri Lanka and Early Career Women Fellowship from the Organization for Women Scientists of Developing Countries, Italy, through a UNESCO grant and the International Development Research Centre, Ottawa, Canada. The views expressed herein do not necessarily represent those of UNESCO, IDRC, or its Board of Governors. The authors would also like to thank Universiti Malaysia Terengganu under Golden Goose Research Grant Scheme (GGRG) (UMT/RMIC/2-2/25 Jld 5 (64), Vot 55191) for supporting Dr. Lam to perform this joint project with the University of Sri Jayewardenepura.

References

- Abedinzadeh, M., Etesami, H., Alikhani, H.A., Shafiei, S., 2020. Combined use of municipal solid waste biochar and bacterial biosorbent synergistically decreases Cd (II) and Pb(II) concentration in edible tissue of forage maize irrigated with heavy metal-spiked water. *Heliyon* 6 (8), e04688.
- Ang, T.N., Young, B.R., Taylor, M., Burrell, R., Aroua, M.K., Baroutian, S.J.C., 2020. Breakthrough analysis of continuous fixed-bed adsorption of sevoflurane using activated carbons 239, 124839.
- Ashiq, A., Adassooriya, N.M., Sarkar, B., Rajapaksha, A.U., Ok, Y.S., Vithanage, M., 2019a. Municipal solid waste biochar-bentonite composite for the removal of antibiotic ciprofloxacin from aqueous media. *J. Environ. Manag.* 236, 428–435.
- Ashiq, A., Sarkar, B., Adassooriya, N., Walpita, J., Rajapaksha, A.U., Ok, Y.S., Vithanage, M., 2019b. Sorption process of municipal solid waste biochar-montmorillonite composite for ciprofloxacin removal in aqueous media. *Chemosphere* 236, 124384.
- Atugoda, T., Wijesekara, H., Werellagama, D., Jinadasa, K., Bolan, N.S., Vithanage, M.J. E.T. and Innovation (2020) Adsorptive interaction of antibiotic ciprofloxacin on polyethylene microplastics: implications for vector transport in water. 100971.
- Bianco, F., Race, M., Papirio, S., Oleszczuk, P., Esposito, G., 2021. The addition of biochar as a sustainable strategy for the remediation of PAH-contaminated sediments. *Chemosphere* 263, 128274.
- Bornemann, L.C., Kookana, R.S., Welp, G., 2007. Differential sorption behaviour of aromatic hydrocarbons on charcoals prepared at different temperatures from grass and wood. *Chemosphere* 67 (5), 1033–1042.
- Carvalho, M.N., da Motta, M., Benachour, M., Sales, D.C.S., Abreu, C.A.M., 2012. Evaluation of BTEX and phenol removal from aqueous solution by multi-solute adsorption onto smectite organoclay. *J. Hazard Mater.* 239–240, 95–101.
- Chen, S., Yue, Q., Gao, B., Li, Q., Xu, X., Fu, K., 2012. Adsorption of hexavalent chromium from aqueous solution by modified corn stalk: a fixed-bed column study. *Bioresour. Technol.* 113, 114–120.
- Chin, C.-J.M., Shih, L.-C., Tsai, H.-J., Liu, T.-K., 2007. Adsorption of o-xylene and p-xylene from water by SWCNTs. *Carbon* 45 (6), 1254–1260.
- Daifullah, A.A.M., Girgis, B.S., 2003. Impact of surface characteristics of activated carbon on adsorption of BTEX. *Colloid. Surface. Physicochem. Eng. Aspect.* 214 (1), 181–193.
- De Gisi, S., Lofrano, G., Grassi, M., Notarnicola, M., 2016. Characteristics and adsorption capacities of low-cost sorbents for wastewater treatment: a review. *Sustainable Materials and Technologies* 9, 10–40.
- de la Luz-Aunci6n, M., P6rez-Ram6rez, E.E., Mart6n-Hern6ndez, A.L., Garc6a-Casillas, P.E., Luna-B6rcenas, J.G., Velasco-Santos, C.J.D., Materials, R., 2020. Adsorption and kinetic study of Reactive Red 2 dye onto graphene oxides and graphene quantum dots 109, 108002.
- Durmusoglu, E., Taspinar, F., Karademir, A., 2010. Health risk assessment of BTEX emissions in the landfill environment. *J. Hazard Mater.* 176 (1–3), 870–877.
- Edathil, A.A., Pal, P., Kannan, P., Banat, F., 2020. Total organic acid adsorption using alginate/clay hybrid composite for industrial lean amine reclamation using fixed-bed: Parametric study coupled with foaming 94, 102907.
- Fl6rez Men6ndez, J.C., Fern6ndez S6nchez, M.L., S6nchez Uria, J.E., Fernandez Martinez, E., Sanz-Medel, A., 2000. Static headspace, solid-phase microextraction and headspace solid-phase microextraction for BTEX determination in aqueous samples by gas chromatography. *Anal. Chim. Acta* 415 (1), 9–20.
- Gunaratne, V., Ashiq, A., Ramanayaka, S., Wijekoon, P., Vithanage, M., 2019. Biochar from municipal solid waste for resource recovery and pollution remediation. *Environ. Chem. Lett.* 17 (3), 1225–1235.
- Hamdy, A., Mostafa, M.K., Nasr, M.J.E.S., Research, P., 2019. Techno-economic estimation of electroplating wastewater treatment using zero-valent iron nanoparticles: batch optimization, continuous feed, and scaling up studies 26 (24), 25372–25385.
- Hercigonja, R., Rac, V., Rakic, V., Auroux, A., 2012. Enthalpy–entropy compensation for n-hexane adsorption on HZSM-5 containing transition metal ions. *J. Chem. Therm.* 48, 112–117.
- Hwang, O., Lee, S.-R., Cho, S., Ro, K.S., Spiehs, M., Woodbury, B., Silva, P.J., Han, D.-W., Choi, H., Kim, K.-Y., Jung, M.-W., 2018. Efficacy of different biochars in removing odorous volatile organic compounds (VOCs) emitted from swine manure. *ACS Sustain. Chem. Eng.* 6 (11), 14239–14247.
- Inyinbor, A., Adekola, F., Olatunji, G.A.J.W.R., Industry, 2016. Kinetics, isotherms and thermodynamic modeling of liquid phase adsorption of Rhodamine B dye onto Raphia hookeri fruit epicarp 15, 14–27.
- Jain, R.K., Cui, Z.C., Domen, J.K., 2016. Environmental Impact of Mining and Mineral Processing. In: Jain, R.K., Cui, Z.C., Domen, J.K. (Eds.). Butterworth-Heinemann, Boston, pp. 53–157.
- Jayawardhana, Y., Gunatilake, S.R., Mahatantila, K., Ginige, M.P., Vithanage, M., 2019a. Sorptive removal of toluene and m-xylene by municipal solid waste biochar: simultaneous municipal solid waste management and remediation of volatile organic compounds. *J. Environ. Manag.* 238, 323–330.
- Jayawardhana, Y., Gunatilake, S.R., Mahatantila, K., Ginige, M.P., Vithanage, M., 2019b. Sorptive removal of toluene and m-xylene by municipal solid waste biochar: simultaneous municipal solid waste management and remediation of volatile organic compounds. *J. Environ. Manag.* 238, 323–330.
- Jayawardhana, Y., Gunatilake, S.R., Mahatantila, K., Ginige, M.P., Vithanage, M., 2019c. Sorptive removal of toluene and m-xylene by municipal solid waste biochar: simultaneous municipal solid waste management and remediation of volatile organic compounds. *J. Environ. Manag.* 238 (September 2018), 323–330.
- Jayawardhana, Y., Kumarathilaka, P., Mayakaduwa, S., Weerasundara, L., Bandara, T., Vithanage, M., 2018. Characteristics of Municipal Solid Waste Biochar: its Potential to Be Used in Environmental Remediation. In: Ghosh, S.K. (Ed.). Springer Singapore, Singapore, pp. 209–220.
- Jayawardhana, Y., Mayakaduwa, S.S., Kumarathilaka, P., Gamage, S., Vithanage, M., 2019d. Municipal solid waste-derived biochar for the removal of benzene from landfill leachate. *Environ. Geochem. Health* 41 (4), 1739–1753.
- Jiang, X., Ouyang, Z., Zhang, Z., Yang, C., Li, X., Dang, Z., Wu, P., 2018. Mechanism of glyphosate removal by biochar supported nano-zero-valent iron in aqueous solutions. *Colloid. Surface. Physicochem. Eng. Aspect.* 547, 64–72.
- Keerthan, S., Bhatnagar, A., Mahatantila, K., Jayasinghe, C., Ok, Y.S., Vithanage, M.J. E.T., Innovation, 2020a. Engineered tea-waste biochar for the removal of caffeine, a model compound in pharmaceuticals and personal care products (PPCPs). from aqueous media 100847.
- Keerthan, S., Rajapaksha, S.M., Trakal, L., Vithanage, M., 2020b. Caffeine removal by *Gliricidia sepium* biochar: influence of pyrolysis temperature and physicochemical properties. *Environ. Res.* 189, 109865.
- Konggidinata, M.L., Chao, B., Lian, Q., Subramaniam, R., Zappi, M., Gang, D.D., 2017. Equilibrium, kinetic and thermodynamic studies for adsorption of BTEX onto Ordered Mesoporous Carbon (OMC). *J. Hazard Mater.* 336, 249–259.
- Krcmar, D., Tenodi, S., Grba, N., Kerkez, D., Watson, M., Roncovic, S., Dalmacija, B., 2018. Preremedial assessment of the municipal landfill pollution impact on soil and shallow groundwater in Subotica, Serbia. *Sci. Total Environ.* 615, 1341–1354.
- Kulikowska, D., Klimiuk, E., 2008. The effect of landfill age on municipal leachate composition. *Bioresour. Technol.* 99 (13), 5981–5985.
- Kumarathilaka, P., Jayawardhana, Y., Basnayake, B.F.A., Mowjood, M.I.M., Nagamori, M., Saito, T., Kawamoto, K., Vithanage, M., 2016. Characterizing volatile organic compounds in leachate from Gohagoda municipal solid waste dumpsite, Sri Lanka. *Groundwater for Sustainable Development* 2–3, 1–6.
- Kumarathilaka, P., Wijesekara, H., Basnayake, B.F.A., Kawamoto, K., Nagamori, M., Saito, T. and Vithanage, M. (2014) Determination of volatile organic compounds (VOCs) in Gohagoda municipal solid waste landfill leachate, Sri Lanka, Sri Lanka.
- Lehmann, J., Joseph, S., 2015. Biochar for Environmental Management: Science, Technology and Implementation. Routledge.
- Li, Y., Liu, S., Wang, C., Ying, Z., Huo, M., Yang, W., 2020. Effective column adsorption of triclosan from pure water and wastewater treatment plant effluent by using magnetic porous reduced graphene oxide 386, 121942.

- Lima, I.M., McAloon, A., Boateng, A.A., 2008. Activated carbon from broiler litter: process description and cost of production. *Biomass Bioenergy* 32 (6), 568–572.
- Lima, L.F., de Andrade, J.R., da Silva, M.G.C., Vieira, M.G.A., 2017. Fixed bed adsorption of benzene, toluene, and xylene (BTX) contaminants from monocomponent and multicomponent solutions using a commercial organoclay. *Ind. Eng. Chem. Res.* 56 (21), 6326–6336.
- Meckenstock, R.U., Warthmann, R.J., Schafer, W., 2004. Inhibition of anaerobic microbial o-xylene degradation by toluene in sulfidogenic sediment columns and pure cultures. *FEMS Microbiol. Ecol.* 47 (3), 381–386.
- Mitra, S., Roy, P., 2011. BTEX: a serious ground-water contaminant. *Res. J. Environ. Sci.* 5 (5), 394.
- Mowla, D., Karimi, G., Salehi, K., 2013. Modeling of the adsorption breakthrough behaviors of oil from salty waters in a fixed bed of commercial organoclay/sand mixture. *Chem. Eng. J.* 218, 116–125.
- Nair, A.T., Senthilnathan, J., Nagendra, S.M.S., 2019. Emerging perspectives on VOC emissions from landfill sites: impact on tropospheric chemistry and local air quality. *Process Saf. Environ. Protect.* 121, 143–154.
- Noufel, K., Djebri, N., Boukhalfa, N., Boutahala, M., Dakhouche, A., 2020. Removal of bisphenol A and trichlorophenol from aqueous solutions by adsorption with organically modified bentonite, activated carbon composites: a comparative study in single and binary systems. *Groundwater for Sustainable Development* 100477.
- Nourmoradi, H., Khiadani, M., Nikaeen, M., 2013. Multi-component adsorption of benzene, toluene, ethylbenzene, and xylene from aqueous solutions by montmorillonite modified with tetradecyl trimethyl ammonium bromide. *J. Chem.* 2013, 589354.
- Nourmoradi, H., Nikaeen, M., Khiadani, M., 2012. Removal of benzene, toluene, ethylbenzene and xylene (BTEX) from aqueous solutions by montmorillonite modified with nonionic surfactant: equilibrium, kinetic and thermodynamic study. *Chem. Eng. J.* 191, 341–348.
- Pavia, D.L., Lampman, G.M., Kriz, G.S., Vyvyan, J.A., 2008. *Introduction to Spectroscopy*. Cengage Learning.
- Rajaratnam, N., Arunachalam, T., Raja, S., Selvasembian, R., 2020. Fenalan Yellow G adsorption using surface-functionalized green nanoceria: an insight into mechanism and statistical modelling. *Environ. Res.* 181, 108920.
- Ramanayaka, S., Vithanage, M., Alessi, D., Liu, W.-J., Jayasundera, A.C.A., Ok, N., 2020. Nanobiochar: production, properties, and multifunctional applications.
- Ranck, J.M., Bowman, R.S., Weeber, J.L., Katz, L.E., Sullivan, E.J., 2005. BTEX removal from produced water using surfactant-modified zeolite. *J. Environ. Eng.* 131 (3), 434–442.
- Rincón-Silva, N.G., Moreno-Piraján, J.C., Giraldo, L.G., 2015. Thermodynamic study of adsorption of phenol, 4-chlorophenol, and 4-nitrophenol on activated carbon obtained from Eucalyptus seed. *Journal of Chemistry* 2015.
- Saiz-Rubio, R., Balseiro-Romero, M., Antelo, J., Díez, E., Fiol, S., Macías, F., 2019. Biochar as low-cost sorbent of volatile fuel organic compounds: potential application to water remediation. *Environ. Sci. Pollut. Control Ser.* 26 (12), 11605–11617.
- Scheutz, C., Mosbaek, H., Kjeldsen, P., 2004. Attenuation of methane and volatile organic compounds in landfill soil covers. *J. Environ. Qual.* 33 (1), 61–71.
- Shimadzu, 2013. *Analysis of VOCs in water using headspace-GC/MS (application note No: LAAN-J-MS-E076)*. Retrieved from Shimadzu corporation website. https://www.shimadzu.com/an/sites/shimadzu.com.an/files/pim/pim_document_file/applications/application_note/10145/jpo212206.pdf.
- Shirani, Z., Song, H., Bhatnagar, A., 2020. Efficient removal of diclofenac and cephalexin from aqueous solution using *Anthriscus sylvestris*-derived activated biochar, p. 140789.
- Silva, B., Martins, M., Rosca, M., Rocha, V., Lago, A., Neves, I.C., Tavares, T.J.S., Technology, P., 2020. Waste-based biosorbents as cost-effective alternatives to commercial adsorbents for the retention of fluoxetine from water 235, 116139.
- Singh, D.K., Kumar, V., Mohan, S., Bano, D., Hasan, S., 2017. Breakthrough curve modeling of graphene oxide aerogel packed fixed bed column for the removal of Cr (VI) from water 18, 150–158.
- Sivarajasekar, N., Baskar, C., 2019. Adsorption of Basic Magenta II onto H₂SO₄ activated immature *Gossypium hirsutum* seeds: kinetics, isotherms, mass transfer, thermodynamics and process design 12 (7), 1322–1337.
- Soria, A.C., García-Sarrió, M.J., Sanz, M.L., 2015. Volatile sampling by headspace techniques. *Trac. Trends Anal. Chem.* 71, 85–99.
- Tham, Y.J., Latif, P.A., Abdullah, A.M., Shamala-Devi, A., Taufiq-Yap, Y.H., 2011. Performances of toluene removal by activated carbon derived from durian shell. *Bioresour. Technol.* 102 (2), 724–728.
- Tran, H.N., Wang, Y.-F., You, S.-J., Chao, H.-P.J.P.S., Protection, E., 2017. Insights into the mechanism of cationic dye adsorption on activated charcoal: the importance of π - π interactions 107, 168–180.
- U.S.EPA (2001) *Cost analyses for selected groundwater cleanup projects: pump and treat systems and permeable reactive barriers*.
- Wibowo, N., Setyadi, L., Wibowo, D., Setiawan, J., Ismadji, S., 2007. Adsorption of benzene and toluene from aqueous solutions onto activated carbon and its acid and heat treated forms: influence of surface chemistry on adsorption. *J. Hazard Mater.* 146 (1–2), 237–242.
- Wijesekara, H.R., De Silva, S.N., Wijesundara, D.T.D.S., Basnayake, B.F.A., Vithanage, M. S.J.E.t, 2015. Leachate plume delineation and lithologic profiling using surface resistivity in an open municipal solid waste dumpsite. *Sri Lanka For.* 36 (23), 2936–2943.
- Yaghmaien, K., Hadei, M., Hopke, P., Gharibzadeh, S., Kermani, M., Yarahmadi, M., Emam, B., Shahsavani, A., 2019. Comparative health risk assessment of BTEX exposures from landfills, composting units, and leachate treatment plants. *Air Quality. Atmosphere & Health* 12 (4), 443–451.
- Yeh, C.-H., Lin, C.-W., Wu, C.-H., 2010. A permeable reactive barrier for the bioremediation of BTEX-contaminated groundwater: microbial community distribution and removal efficiencies. *J. Hazard Mater.* 178 (1), 74–80.
- Yue, Z., Mangun, C., Economy, J., Kemme, P., Cropek, D., Maloney, S., 2001. Removal of chemical contaminants from water to below USEPA MCL using fiber glass supported activated carbon filters. *Environ. Sci. Technol.* 35 (13), 2844–2848.
- Zhang, C., Li, F., Guo, G., Teng, Y., Zhang, Z., 2016. Risk assessment of BTEX in the groundwater of songyuan region of songhua river in China. *Water Supply* 16 (1), 135–143.
- Zhang, Y., Xu, X., Cao, L., Ok, Y.S., Cao, X., 2018. Characterization and quantification of electron donating capacity and its structure dependence in biochar derived from three waste biomasses. *Chemosphere* 211, 1073–1081.
- Zhou, Q., Jiang, X., Li, X., Jia, C.Q., Jiang, W., 2018. Preparation of high-yield N-doped biochar from nitrogen-containing phosphate and its effective adsorption for toluene. *RSC Adv.* 8 (53), 30171–30179.